MALAYSIAN JOURNAL OF SCIENCE
MJS
ISSN 1394-3065

Regular Issue

Malaysian Journal of Science 44 (2): 78-85 (June 2025) https://mjs.um.edu.my

# Effect of Cu and Si Wafer Substrates in Increasing Raman Signal of Surface-Enhanced Raman Scattering-Based Au Nanoparticles

Affi Nur Hidayah[1ab], Djoko Triyono[2a]*, Yuliati Herbani[3b] and Rosari Saleh[4a]

**Abstract:** Surface-enhanced Raman spectroscopy (SERS) has attracted considerable research interest over the last four decades because of its rapid vibrational spectroscopic detection, high sensitivity, and nondestructive technique for enhancing the generally weak signal from Raman scattering. Here, SERS substrates were fabricated by drop-casting Au nanoparticles (NPs) onto two substrates (Cu and Si wafers). The AuNPs (diameter = 7.3 nm) were synthesized from an Au metal ion solution with a concentration of $4.22 \times 10^{-4}$ M via photochemical reduction using a femtosecond laser. The SERS substrates were tested for their ability to enhance the Raman signal of paraquat pesticides at 10 ppm. Six vibration peaks of the paraquat pesticides at 671, 838, 1187, 1294, 1530, and 1643 $cm^{-1}$ were successfully detected and enhanced. The results showed that the SERS substrate on the Si wafer increased the Raman signal more than the Cu wafer.

***Keywords:*** *SERS substrates, Au nanoparticles, silicon wafer, copper wafer.*

## 1. Introduction

The unique chemical, physical, optical, catalytic, and electronic capabilities of metallic nanoparticles (NPs) have attracted significant research attention because these properties are influenced by plasmonic oscillations. The plasmonic oscillations of metal NPs strongly rely on various variables, such as the material, size, shape, nanostructure composition, and the dielectric constant of the surrounding medium (Minho, Jung-Hoon & Jwa-Min, 2019). Plasmon resonance exhibits sensitivity toward alterations in the refractive index of the surrounding medium, which can arise from the adsorption or binding of molecules onto material surfaces. This property renders plasmon resonance valuable for the development of environmental sensing applications, including colorimetry (Xu, Jin & Li, 2021), surface-enhanced Raman scattering (SERS) (Israelsen, Hanson, and Vargis, 2015), and biosensing applications (Unser, Bruzas, He & Sagle, 2015) (Huan et al, 2021).

SERS has been developed as a straightforward and nondestructive testing method for the detection of dangerous chemical substances and food contaminants, e.g., antibiotics, melamine, and pesticides (Craig, Franca, & Irudayaraj, 2013). In addition, SERS has demonstrated its efficacy in detecting various biological entities, such as micro-RNA, DNA, viruses, bacteria, and cancer cells (Pilot et al., 2019). Noble metallic elements, including Au, Ag, and Cu, are commonly utilized in the form of metal NPs for SERS-substrate modification (Roguska et al., 2011). In a study by Wang, K G et al. (2019), AgNPs exhibited sharp and narrow plasmon peaks, resulting in a high intensity. This characteristic enabled the AgNPs to more effectively amplify the Raman signal compared with AuNPs. Nevertheless, Ag is highly susceptible to oxidation and exhibits potentially harmful characteristics that can adversely affect the analyte under investigation (Ferdous & Nemmar, 2020). AuNPs have attracted significant attention in the medical field because of their remarkable biocompatibility (Janina et al., 2010). This interest has been further fueled by the high plasmonic stability of Au attributed to its elevated chemical and physical stability (Ilyas et al., 2021) (Hidayah et al., 2022).

The use of SERS substrates has been demonstrated to enhance the typically low signal strength obtained from Raman spectroscopy. This enhancement occurs when biomolecules, which are the targets or analytes for environmental pollution, interact with the plasmonic nanostructures on the substrate surface (Pérez-Jiménez et al., 2020). The plasmonic oscillation of metal NPs can manifest in two separate effects. Initially, the phenomenon of extinction or scattering results in a displacement of the spectral peak toward long wavelengths. It has been observed that plasmonic nanostructures can increase nonelastic optical phenomena on molecules or quantum entities through local field enhancement (Lia, Cushinga & Wua, 2015). Surface plasmons (SPs), specifically localized SPs at the metal surface, interact with incident photons and Raman-scattered vibrations emitted by analyte molecules. These interactions result in a substantial enhancement of Raman-scattered photons,

**Authors information:**
[a]School Department of Physics, Universitas Indonesia, Kampus UI Depok, INDONESIA. E-mail: djoko.triyono@sci.ui.ac.id[2]; rosari.saleh@ui.ac.id[4]
[b]Research Center for Photonics, National Research and Innovation Agency, Kawasan PUSPIPTEK Building 442, Tangerang Selatan 15314, INDONESIA. E-mail: affi001@brin.go.id[1]; yuli018@brin.go.id[3]
*Corresponding Author: djoko.triyono@sci.ui.ac.id

Received: June, 2023
Accepted: June, 2024
Published: June, 2025



DOI:https//doi.org/10.22452/mjs.vol44no2.8
Malaysian Journal of Science 44(2): 78-85 (June 2025)

commonly known as electromagnetic enhancement (EM). Chemical enhancement (CM) can yield additional performance enhancements when the molecule establishes a chemical bond with the metal surface, leading to the transfer of charge, involving the metal and molecule. The aforementioned processes are considered the basis for SERS (Kahraman et al., 2017).

AuNPs are a popular choice for SERS substrates. However, the shape of the NPs (Au nanospheres, nanorods, nanotriangles, nanowires, nanoplates, and nanocubes), substrate type (Si, glass, quartz, and paper), and analyte used impacts the process of increasing the Raman signal on an AuNP SERS substrate (Lopez-Lorente, 2021). Numerous AuNPs that are used as SERS substrates are still produced using chemical reduction techniques that involve reducing agents, such as stainless steel (Lopez-Lorente, 2014), trisodium citrate (Brust, 1994), $NaBH_4$, or ascorbic acid (Saim, 2021). The chemical reduction approach is complicated and can result in chemical residues on the AuNPs, which could be harmful if utilized in medical applications. Thus, using a femtosecond laser to create AuNPs via the chemical photoreduction process could be beneficial because it is simpler, faster, and does not require chemicals.

AuNP SERS substrates have been used to detect a range of analytes, including pesticides, such as phosmet (Luo, 2016), carbaryl (Alsammarraie, 2017), thiram (Zhang, 2014), cypermethrin (Li, 2019), esfenvalerate (Wang, K., 2019), pestisida thiabendazole (Alsammarraie, 2018) and paraquat pesticides. Currently, chemical reduction to fabricate AuNPs is the only approach used for AuNP-based SERS substrates in the detection of pesticides. There are several methods for performing the SERS-substrate measurement process for detecting paraquat pesticides. They include combining the pesticide with AuNPs and dropping them onto a glass substrate (Lin, 2021), aluminum engraved using a laser and coating with AuNPs (Kamkrua, 2023), or dropping AuNPs onto glass and drying in a vacuum oven for 6 h (Chen, 2022). No reports have been made regarding the production of SERS substrates on Cu and Si wafers for the detection of paraquat pesticides. Although the use of paraquat insecticide has begun to be outlawed in Europe and America, farmers in Indonesia continue to use it. Paraquat pesticides are commonly used by farmers to kill pests on coffee and oil palm trees (Pusat Standarisasi-Kementerian Lingkungan Hidup dan Kehutanan, 2020). Thus, the advancement of the field of spectroscopy in Indonesia is critically dependent on the development of a SERS substrate based on AuNPs.

The fabrication techniques employed for the production of SERS substrates include spin coating (Gushiken et al., 2020), electron beam lithography (Chen et al., 2019), and physical vapor deposition (Khalil et al., 2019). Nevertheless, it might be argued that the aforementioned methods are highly complex, difficult, and costly. The quality of SERS substrates can impact SERS signals. The present study fabricated SERS substrates by the application of a drop-casting technique, which was confirmed to be rapid and cost-effective. AuNPs were used as the primary material, and they were coated onto Cu and Si wafers. The initial step in the production of the AuNPs involves the use of a femtosecond laser for photochemical reduction, commonly referred to as the green synthesis method. This approach prevents the use of strong chemical reduction agents. The AuNPs were produced by diluting Au salts in a water solution, placing them in a glass cuvette, and irradiating them using the femtosecond laser. When a femtosecond laser interacts with a solution of Au ions, it generates a strong reducing agent that can convert Au ions into AuNPs. This study was aimed at evaluating the impact of various substrate types on the enhancement of the Raman signal of paraquat pesticides.

## 2. Materials and Methods

### Materials

An AuNP solution was synthesized by reducing a solution of Au ions using the femtosecond laser. The Au ion solution was prepared by diluting potassium gold (III) chloride metal salt ($KAuCl_4$; 98% purity, Sigma Aldrich) with distilled water to a concentration of $4.22 \times 10^{-4}$ M. Furthermore, a capping agent, polyvinylpyrrolidone (PVP; 99.9% purity, Sigma Aldrich), was utilized. The PVP had a molecular weight of 40,000 incorporated into the solution at a concentration of 0.01 wt%.

Paraquat pesticides (Sigma Aldrich) were selected as analytes for the quality testing of the present SERS substrates. The paraquat pesticide (1 g) was diluted multiple times to achieve a concentration of 10 ppm.

### Methods

The AuNP SERS substrates were fabricated on two distinct substrates: Si and Cu wafers. The AuNPs were first produced via a photoreduction process with a femtosecond laser and subsequently placed on the wafers to create SERS substrates using the drop-casting method. The use of a femtosecond laser created NPs without chemicals or strong reduction agents, offering a rapid and more eco-friendly alternative to chemical techniques.

To synthesize colloidal AuNPs, a solution containing Au ions was introduced into a quartz cuvette (10 × 10 × 45 mm), resulting in a total volume of 3 mL. The solution was subsequently exposed to a femtosecond laser, with a fundamental wavelength of 800 nm, power output of 2 mJ, and repetition rate of 1 kHz. The experiment was conducted for 15-min irradiation times. The laser beam was directed at a right angle to the side wall of the glass cuvette using an aspheric lens (numerical aperture = 0.5; focal length = 8 mm). The schematic representation of the experimental setup has been previously illustrated (Hidayah et al., 2022). After the irradiation process, the ultraviolet–visible (UV–VIS) absorption of the synthesized AuNPs was analyzed using a modular UV–VIS spectrophotometer (Maya2000 Pro) and a broadband light source (DH-Mini, Ocean Optics). The colloidal AuNPs were deposited on grids with a carbon coating (Ted Pella, Inc.) and allowed to dry for at least 24 h. Afterward, their morphology was investigated via transmission electron microscopy (TEM) (FEI Tecnai G2 20 S-Twin) at an acceleration voltage of 200 kV.

The SERS substrates were fabricated by drop casting the


DOI:https//doi.org/10.22452/mjs.vol44no2.8
Malaysian Journal of Science 44(2): 78-85 (June 2025)

colloidal AuNPs (1 mL) onto the Si wafers and Cu substrates (0.5 × 0.5 cm) placed on a hot plate at 40°C. The hot plate was set to 40°C to minimize coffee ring formation and alterations in the characteristics of the AuNPs. Prior to a quality assessment of the SERS substrate, normal Raman spectra of the standard paraquat pesticide were evaluated. The paraquat pesticide (2 µL, 10 ppm) was dropped onto the SERS Cu and Si substrates, which were dried at room temperature. SERS experiments were conducted using a Raman spectrometer with a 785-nm excitation source and gratings of 1800 grooves per millimeter (HR 550, Horiba). Figure 1 illustrates the production of the SERS substrate and the measurement using Raman spectroscopy.

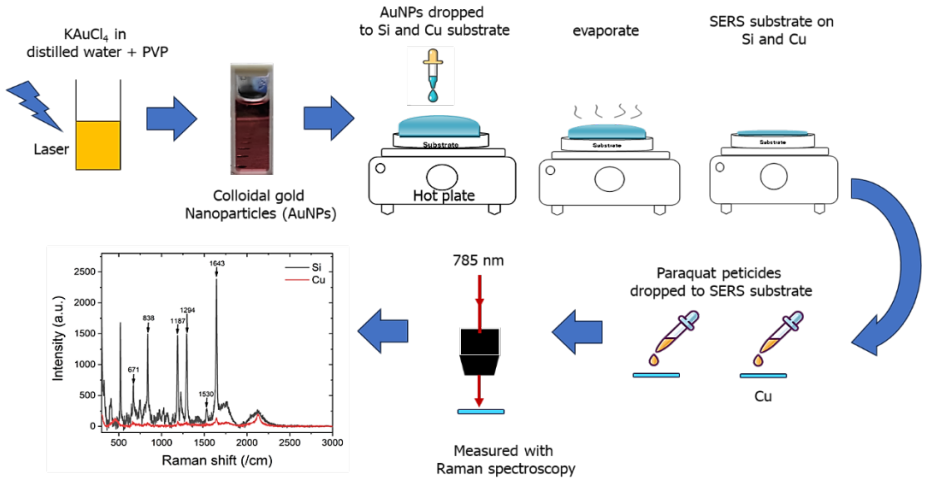


**Figure 1.** Production of SERS substrates and Raman measurements.

## 3. Results and Discussion

First, the AuNPs were generated from a solution of Au ions, which were placed in cuvettes and exposed to a femtosecond laser for 15 min. This was performed prior to the production of SERS substrates on Si and Cu wafers. The femtosecond laser was used to irradiate the Au ion solution, which is a mixture of water ($H_2O$) and $K^+[AuCl4]^-$. The interaction between the $H_2O$ and the tightly focused laser created plasmas containing reactive radicals, such as hydrated electrons ($e^-_{aq}$-), hydrogen peroxide ($H_2O_2$), and hydroxyl radicals (OH). The hydrogen radicals and hydrated electrons acted as strong reducing agents and reduced $K^+[AuCl_4]^-$ to AuNPs (Meader et al, 2017).

The absorbance of the AuNP solution was measured, and the findings are illustrated in Figure 2, depicting the localized surface plasmon resonance (LSPR) value at 522 nm. Furthermore, the NPs were characterized by TEM, and the results are shown in Figure 3, illustrating the spherical morphology of the NPs with a diameter of 7.3 nm.

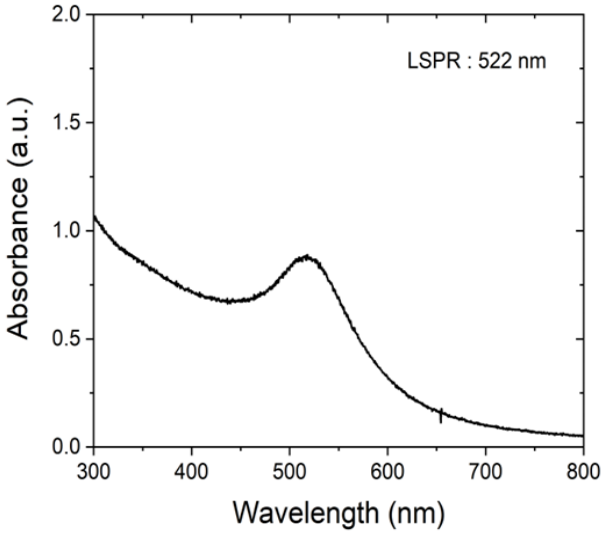


**Figure 2.** Localized surface plasmon resonance of AuNPs.


DOI:https//doi.org/10.22452/mjs.vol44no2.8
Malaysian Journal of Science 44(2): 78-85 (June 2025)

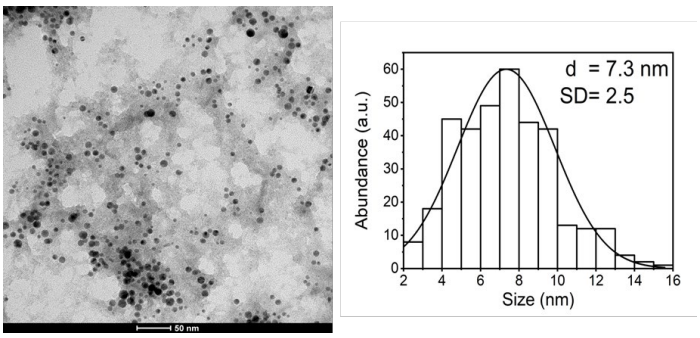


**Figure 3.** TEM images of morphology and particle size of AuNPs.

The colloidal AuNPs were subsequently coated onto the Si and Cu wafers, respectively, using a hot plate. The Si SERS substrate was characterized via field-emission scanning electron microscopy (FE-SEM; Figure 4).

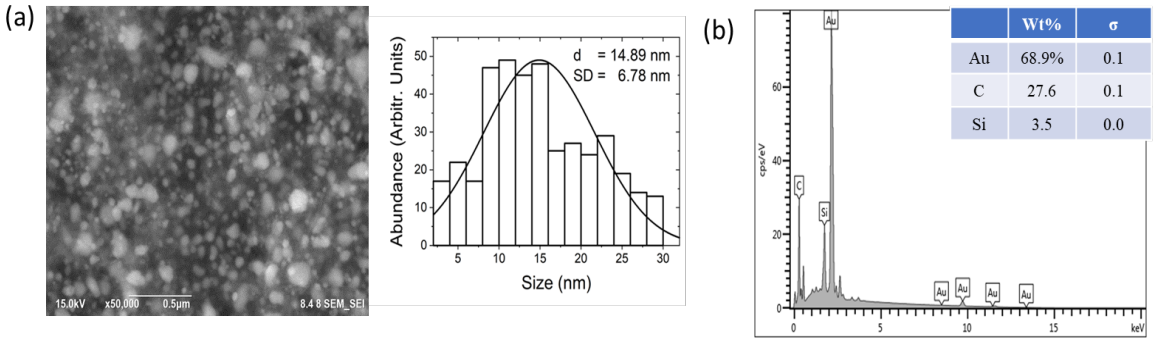


**Figure 4.** (a) FE-SEM images of the morphology and particle size. (b) Energy-dispersive X-ray spectroscopy.

The experimental findings indicated that AuNPs, when applied as a coating on a Si wafer substrate, were larger than the NPs in the solution suspension. This implies that the transfer mechanism of the colloidal AuNPs onto the substrate, in conjunction with the impact of the temperature of the hot plate, resulted in the heightened aggregation and enlargement of the NPs. The weight percentage of the NPs successfully coated on the Si wafer substrate was 68.9%. When colloidal AuNPs are deposited on a substrate and evaporate, the capillary flow from the center to the edge within the droplets causes the NPs to aggregate at the edge of the droplet, leading to their cohesion (Kumar, 2020). The van der Waals interaction between the NPs and heating on the hot plate accelerated the evaporation process, leading to a faster aggregation of the NPs. Once the NPs were adhered to the substrate, the heating process continued in the thin film. The heat produced by the hot plate follows principles, such as the annealing process on thin films. This process involves heating to enhance the crystallinity of the film and enlarges the size of NPs in the thin film (Kabir, 2019). This technique results in a coffee ring effect, causing the particles to be more concentrated at the edges than in the middle (Eral, 2013).

Standard paraquat pesticide powder ($C_{12}H_{14}Cl_2N_2$; Sigma Aldrich) was subjected to Raman spectroscopy prior to evaluating the quality of the SERS substrate. Six signal peaks corresponding to the paraquat pesticide were observed in the Raman spectrum (Figure 5) at the following wave numbers: 654.87, 841.87, 1199.29, 1300.54, 1552.08, and 1655.5 $cm^{-1}$.

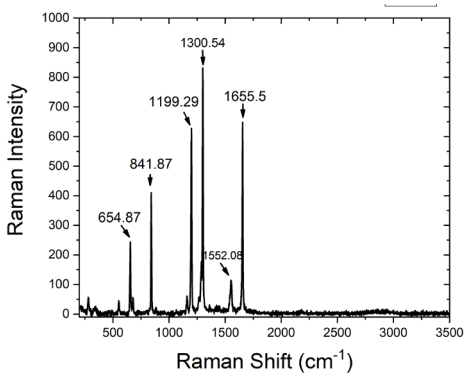


**Figure 5.** Raman shift of standard paraquat pesticide powder.


DOI:https//doi.org/10.22452/mjs.vol44no2.8
Malaysian Journal of Science 44(2): 78-85 (June 2025)

The quality testing of the SERS substrates was conducted on Si and Cu wafers. A droplet (2 µL) of paraquat pesticide solution was applied to each substrate, which was subsequently dried at room temperature. To assess the efficacy of the AuNPs in enhancing the Raman signal of paraquat pesticides, two sets of measurements were conducted. The first set involved an empty Si wafer substrate devoid of NPs and pesticides. The second set involved an empty Si substrate without NPs, onto which the paraquat pesticide (2 µL) was applied; the substrate was subsequently dried at room temperature. Figure 6 shows a comparative analysis of Raman signal outcomes from three samples: empty Si wafer substrates, Si wafers without NPs treated with paraquat pesticides, and SERS substrates treated with pesticides.

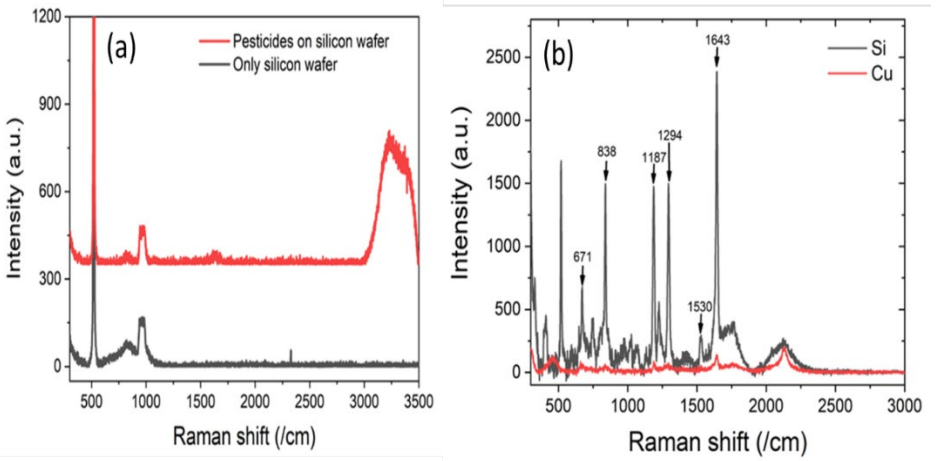


**Figure 6.** Raman shifts of (a) only Si wafer, pesticides on Si wafer, and (b) pesticides on SERS substrate on Si and Cu wafers.

The Raman spectroscopy of a blank Si wafer revealed distinct peaks at 500 and 1000 $cm^{-1}$ (Figure 6a). No Raman peaks resulting from paraquat pesticides were observed for the uncoated Si wafer substrate and the Si wafer substrate that was not treated with NPs and pesticides. Here, the use of SERS substrates on Si and Cu wafers enhanced the detection of six distinct paraquat pesticide peaks. These peaks were observed at 671, 838, 1187, 1294, 1530, and 1643 $cm^{-1}$, which represent the C–Cl stretching vibration, C–N stretching vibration, C=C symmetrical stretching vibration, C–C deformation vibration, C–C deformation vibration, and C=N stretching vibration (Chen, 2022). This showed that the presence of NPs with plasmonic characteristics on the SERS substrate enabled the modulation and interaction of electromagnetic waves, Raman scattering, with the molecular vibrations of paraquat pesticides. Six paraquat pesticide peaks of the Raman shift observed for the SERS substrate exhibited slight deviations compared with the Raman spectra obtained for powdered paraquat pesticide. These deviations were attributable to the impact of plasmonic interactions occurring on the NPs. This influenced the enhancement of the incident laser source and the vibrational behavior of the paraquat pesticide molecules, contrary to the molecular vibrations of powdered paraquat pesticides, which were only affected by the laser source passing through the molecule (Liao, 2007).

The observed enhancement in the Raman signal of the paraquat insecticide on the SERS Si substrate was greater than that on the Cu substrate. The SERS enhancement factor (EF) combines two multiplicative contributions from CM and EM. Thus, the augmentation of the Raman signal was influenced by both EM and CM. This experiment evaluated the efficacy of the SERS substrate using the paraquat pesticide as the analyte. Two distinct substrate types were used to assess the quality of the SERS substrate. In this experiment, the EM process influenced the enhancement of the Raman signal of the paraquat pesticides more than the CM because the amplification of the Raman signal was solely influenced by the plasmonic properties of the NPs. The plasmonic characteristics exhibited by AuNPs coated on a Si wafer substrate are governed by the surface plasmon polariton (SPP) phenomenon. This effect is governed by the dielectric properties of the substrate in which the NPs are implanted (Le Ru, 2009).

SPP signals can be amplified using different methods depending on the material used. The dielectric value of the material had an effect on the SPP by strengthening the Raman signals. Once NPs are placed on the SERS substrate, LSPR and polaritons begin to form. Polaritons are caused by electron oscillations moving through the substrate material. The material can strengthen the electric field around the NPs owing to polaritons. Plasmon effects that increase electromagnetic waves are caused by SPP and the interaction between NPs and the dielectric constant of the


DOI:https//doi.org/10.22452/mjs.vol44no2.8
Malaysian Journal of Science 44(2): 78-85 (June 2025)

substrate. To determine the field on the SERS material, lasers with electric fields of EInc to the polariton mode were used. The Raman signal enhancement was affected by the factor, MLoc = |ELoc/EInc|, for increasing the local field strength (LFIEF). The electric field of the SERS ELoc substrate is changed by the polariton electric field, which works with the dielectric electric field ($E_1$) and metal electric field ($E_2$). The factor for increasing the LFIEF was determined using the following equation:

$$M = \frac{|E_1(0)|^2}{|E_{Inc}(0)|^2} = \frac{2|\epsilon|}{\epsilon_M \epsilon''} I_m \left(\epsilon \sqrt{\frac{1}{\epsilon + \epsilon_M}}\right) \eta \sqrt{\epsilon_{Inc} cos_{\theta_{Inc}}}, \quad (1)$$

where $E_{Inc}$ is the electric field of the laser, $\epsilon_{Inc}$ is the dielectric where the wave arrives, $\theta_{Inc}$ is the angle of incidence, Im is the imaginary part, ϵ is the substrate dielectric, ϵ'' is the imaginary substrate dielectric, and $\epsilon_M$ is the medium dielectric (Le Ru, 2009). The dielectric constant of the SERS substrate impacts signal growth and the EF value.

The Raman signal amplification on the Si wafer substrate exceeded that on the Cu substrate, mostly attributable to the disparity in dielectric constants. The dielectric constant of the Si wafer substrate (11.7) exceeded that of the Cu substrate (1.68). The Si wafer substrate, with its higher dielectric constant, had a higher influence on the plasmonic characteristics of the SERS substrate. The stronger plasmonic coupled and increased the Raman vibration of the pesticide molecules, as represented by the higher Raman peak compared with that of the SERS Cu substrate. The EF for the SERS Si substrate was $2.38 \times 10^4$, higher than that for the Cu substrate ($1.39 \times 10^2$). The EF is determined using (ISERS/IRaman) × (NRaman/NSERS), where ISERS represents the SERS intensity, IRaman is the standard Raman intensity, NRaman is the analyte concentration in standard Raman measurements, and NSERS is the analyte concentration in SERS measurements (Ru, 2013).

## 4. Conclusion

This study effectively fabricated SERS substrate-based AuNPs on Si and Cu wafer substrates. The SERS substrates were fabricated via the drop-casting method, and AuNPs (diameter = 7.3 nm), synthesized from Au metal salts dissolved in water and irradiated with a femtosecond laser, were deposited onto both substrates. The quality assessment of the SERS substrate relied on its ability to enhance the Raman signal of the paraquat pesticides. The experimental findings showed that the AuNPs could enhance the Raman signal, leading to the successful detection of six Raman peaks associated with the paraquat insecticide. The SERS substrate on a Si wafer significantly amplified the Raman signal for the paraquat insecticide compared with the Cu substrate. This was due to the higher dielectric constant of the Si wafer than that of the Cu wafer. The higher dielectric constant influenced the behavior of the localized SPPs, facilitating the coupling of the Raman scattering vibrations of the paraquat pesticide molecules. Further investigation is required to investigate the impact of other substrates, in addition to Si and Cu wafers, on the amplification of Raman signals for analytes under examination.

## 5. Acknowledgement

This paper was supported by Rumah Program ORNM Badan Riset dan Inovasi Nasional and Universitas Indonesia under Grant PUTI NKB-4502/UN2.RST/HKP.05.00/2020.

## 6. References

Alsammarraie, F K., Lin, M S. (2017). Using standing gold nanorod arrays as surface-enhanced Raman spectroscopy (SERS) substrates for detection of carbaryl residues in fruit juice and milk. J. Agric. Food Chem. 65 : 666−674.

Alsammarraie, F K., Lin, M S., Mustapha, A., Lin, H T., Chen, X., Chen, Y H., Wang, H., Huang, M Z. (2018). Rapid determination of thiabendazole in juice by SERS coupled with novel gold nanosubstrates. Food Chem. 259 : 219−225.

Anema J R., Li J F., Yang Z L., Ren B. and Tian Z. Q. (2011). Shell-isolated nanoparticle-enhanced Raman spectroscopy: expanding the versatility of surface-enhanced Raman scattering, Annual Review of Analytical Chemistry 4:129-150.

Brust, M., Walker, M., Bethell, D., Schiffrin, D.J., Whyman, R. (1994). Synthesis of thiolderivatised gold nanoparticles in a two-phase Liquid-Liquid system, J. Chem. Soc., Chem. Commun 7 : 801e802.

Chen Y T., Pan L., Horneber A., Berg M., Miao P., Xu P., Adam P M., Meixner A J., and Zhang D. (2019). Charge transfer and electromagnetic enhancement processes revealed in the SERS and TERS of a CoPc thin film, Nanophotonics 8(9), 1533-1546.

Chen, W., Li, C., Yu, Z., Song, Y., Zhang, X., Ni, D., Zhang, D., Liang, P. (2022). Optimum synthesis of cactus-inspired SERS substrate with high roughness for paraquat detection, Spectrochimica Acta Part A: Molecular and Biomolecular Spectroscopy 268 : 120703.

Craig A P., Franca A S., and Irudayaraj J. (2013). Surface-Enhanced Raman Spectroscopy Applied to Food Safety, Annu. Rev. Food Sci. Technol. 4:369–80.

Eral, H., Oh, J. (2013). Contact angle hysteresis: a review of fundamentals and applications, Colloid Polym. Sci. 291 : 247–260.

Ferdous Z. and Nemmar A. (2020). Health Impact of Silver Nanoparticles: A Review of the Biodistribution and Toxicity Following Various Routes of Exposure, Int. J. Mol. Sci. 21(7):2375.

Gushiken N K., Paganoto G T., Temperini M L A., Teixera F S. and Salvadori M C. (2020). Substrate for Surface-Enhanced Raman Spectroscopy Formed by Gold Nanoparticles Buried in Poly (methyl methacrylate), ACS Omega 5(18):10366-10373.



DOI:https//doi.org/10.22452/mjs.vol44no2.8
Malaysian Journal of Science 44(2): 78-85 (June 2025)

Hidayah, A.N., Herbani, Y., Steven, E., Subhan, A., Triyono, D., Isnaeni, Suliyanti, M. M., and Shiddiq, M. (2022). Tuning the electrical properties of colloidal nanoalloys by varying their composition, Colloids and Surfaces A: Physicochemical and Engineering Aspects 641:128496.

Hidayah, A N., Triyono, D., Herbani, Y., and Saleh, R. (2022). Liquid Surface-Enhanced Raman Spectroscopy (SERS) Sensor-Based Au-Ag Colloidal Nanoparticles for Easy and Rapid Detection of Deltemthrin Pesticide in Brewed Tea, Crystals 12:24.

Huan Q., Liu Y., Chang S., Chen H., and Chen J. (2016). Surface Plasmonic Sensors: Sensing Mechanism and Recent Applications, Sensors 21(16):5262.

Ilyas H., Zeeshan T., Sattar N. A., Ramay S. M., Mahmood A., Abbas H. G., Saleem M. (2021). First principle and experimental investigations of monodispersed Au plasmonic nanoparticles on $TiO_2$, Chemical Physics Letters 783:139080.

Israelsen N D., Hanson C. and Vargis E. (2015). Nanoparticles Properties and Synthesis Effects on Surface-Enhanced Raman Scattering Enhancement Factor: An Introduction, The Scientific World Journal 2015: 124582.

Kabir, M H., Ali, M. M., Kaiyum, M A., and Rahman, M S. (2019). Effect of annealing temperature on structural morphological and optical properties of spray pyrolized Al-doped ZnO thin films, J. Phys. Commun. 3 : 105007.

Kahraman M., Mullen E R., Korkmaz A. and Wachsmann-Hogiu S. (2017). Fundamentals and Applications of SERS-based bioanalytical sensing, Nanophotonics 6(5).

Kamkrua, N., Ngernsutivorakul, T., Limwichean, S., Eiamchai, P., Chananonnawathorn, C., Pattanasetthakul, V., Ricco, R., Choowongkomon, K., Horprathum, M., Nuntawong, N., Bora, T., and Botta, R. (2023). Au Nanoparticle-Based Surface-Enhanced Raman Spectroscopy Aptasensors for Paraquat Herbicide Detection, ACS Appl. Nano Mater. 6 : 1072−1082.

Khalil I., Chou C M., Tsai K L., Hsu S., Yehye W A., and Hsiao V K S. (2019). Gold Nanofilm-Coated Porous Silicon as Surface-Enhanced Raman Scattering Substrate, Appl. Sci. 9: 4806.

Kneipp J., Kneipp H., Wittig B., and Kneipp K. (2010). Novel optical nanosensors for probing and imaging live cells, Nanomedicine 6(2):214–226.

Kumar, A K S., Zhang, Y., Li, D., Compton. R G. (2020). A mini-review: How reliable is the drop casting technique?. Electrochemistry Communications 121 : 106867.

Le Ru, E. and Etchegoin P. (2009). Principles of Surface Enhanced Raman Spectroscopy. Pp. 134-135, UK, Oxford: Elsivier.

Le Ru, E C., and Etchegoin, P G. (2013). Quantifying SERS enhancements, MRS (Materials Research Society) Bulletin 38 : 631 – 640.

Lia M., Cushinga S K., and Wua N. (2015). Plasmon-enhanced optical sensors: a review, Analyst 140 (2):386–406.

Liao, Q., Li, M Y., Hao, R., Ai, X C., Zhang, J P., Wang, Y. (2007). Surface-enhanced Raman scattering and DFT computational studies of cyanuric chloride derivative, Vibrational Spectroscopy 4 : 351-356.

Li, X Z., Yang, T Y., Song, Y T., Zhu, J H., Wang, D L., Li, W. (2019). Surface-enhanced Raman spectroscopy (SERS)-based immunochromatographic assay (ICA) for the simultaneous detection of two pyrethroid pesticides. Sens. Actuators, B 283 : 230−238.

Lin, M H., Sun, L., Kong, F., Lin, M. (2021). Rapid detection of paraquat residues in green tea using surface-enhanced Raman spectroscopy (SERS) coupled with gold nanostars, Food Control 130 : 108280.

Lopez-Lorente, A. I., Simonet, B.M., Valc_arcel, NM., Eppler, S., Schindl, R., Kranz, C., Mizaikoff, B. (2014). Characterization of stainless steel assisted bare gold nanoparticles and their analytical potential, Talanta 118 : 321e327.

Lopez-Lorente, A. I. (2021). Recent developments on gold nanostructures for surface enhanced Raman spectroscopy: Particle shape, substrates and analytical applications. A review, Analytica Chimica Acta 1168 : 338474.

Luo, H R., Huang, Y Q., Lai, K Q., Rasco, B A., Fan, Y X. (2016). Surface-enhanced Raman spectroscopy coupled with gold nanoparticles for rapid detection of phosmet and thiabendazole residues in apples. Food Control 68 : 229−235.

Meader V K., John M G., Rodrigues C J., Tibbetts K M. (2017). Roles of Free Electrons and H2O2 in the Optical Breakdown-Induced Photochemical Reduction of Aqueous [$AuCl_4$], J. Phys. Chem. A 121:6742–6754.

Minho K., Jung-Hoon L., Jwa-Min N. (2019). Plasmonic Photothermal Nanoparticles for Biomedical Applications, *Adv. Sci*. 6:1900471.

Pusat Standarisasi Instrumen Kualitas Lingkungan Hidup, Kementerian Lingkungan Hidup dan Kehutanan Republik Indonesia. (2020). *Konversi Rotterdam: Pro dan Kontra Paraquat Dichloride*. Maret 2024. (https://psiklh.bsilhk.menlhk.go.id/v2/?p=11619).

Pérez-Jiménez A I., Lyu D., Lu Z., Liu G., and Ren B. (2020). Surface-enhanced Raman spectroscopy: benefits, trade-offs and future developments, Chem. Sci. 11:4563-4577.



DOI:https//doi.org/10.22452/mjs.vol44no2.8
Malaysian Journal of Science 44(2): 78-85 (June 2025)

Pilot R., Signorini R., Durante C., Orian L. (2019). Manjari Bhamidipati and Laura Fabris, A Review on Surface-Enhanced Raman Scattering, Biosensors 9:57.

Pissuwan D., Camilla G., Mongkolsuk S., Cortie M. B. (2019). Single and multiple detections of foodborne pathogens by gold nanoparticle assays, WIREs Nanomed. Nanobiotechnol. 12:1584.

Roguska A., Kudelski A., Pisarek M., Opara M., and Janik-Czachor M. (2011). Surface-enhanced Raman scattering (SERS) activity of Ag, Au and Cu nanoclusters on $TiO_2$-nanotubes/Ti substrate, Appl. Surf. Sci. 257(19):8182–8189.

Saim, A K., Kumah, F N., Oppong, M N. (2021). Extracellular and intracellular synthesis of gold and silver nanoparticles by living plants: a review, Nanotechnol. Environ. Eng. 6 : 1.

Unser S., Bruzas I., He J. and Sagle L. (2015). Localized Surface Plasmon Resonance Biosensing: Current Chalengges and Aprroaches, Sensors 15(7):15684-15716.

Wang K., Sun D W., Pu H. and Wei Q. (2019). Shell thickness-dependent Au@Ag nanoparticles aggregates for high-performance SERS applications, Talanta 195:506-515.

Wang, K G., Sun, D W., Pu, H B., Wei, Q Y. (2019). Surface enhanced Raman scattering of core-shell Au@Ag nanoparticles aggregates for rapid detection of difenoconazole in grapes. Talanta 191 : 449−456.

Xu N., Jin S., and Li W. (2021). Metal nanoparticles-based nanoplatforms for colorimetric sensing: A review, Reviews in Analytical Chemistry 40: 1–11.

Yonzon C R., Haynes C L., Zhang X., Walsh J T., Van Duyne R P. (2004). A glucose biosensor based on surface-enhanced Raman scattering: improved partition layer, temporal stability, reversibility, and resistance to serum protein interference, *Anal. Chem.* 76(1):78-85.

Zhang D., Pu H., Huang L., and Sun D. (2021). Advances in flexible surface-enhanced Raman scattering (SERS) substrates for nondestructive food detection: Fundamentals and recent applications, *Trends in Food Science & Technology* 109:690-701.

Zhang, Y Z., Wang, Z Y., Wu, L., Pei, Y W., Chen, P., Cui, Y P. (2014). Rapid simultaneous detection of multi-pesticide residues on apple using SERS technique. Analyst 139 : 5148−5154.

Zhao Y., Gan S., Zhang G., Dai X. (2019). High sensitivity refractive index sensor based on surface plasmon resonance with topological insulator, Results in Physics 14:102477.



DOI:https//doi.org/10.22452/mjs.vol44no2.8
Malaysian Journal of Science 44(2): 78-85 (June 2025)